IRAQI BULLETIN OF GEOLOGY AND MINING (IBGM)\
IRAQ GEOLOGICAL SURVEY (GEOSURV-IRAQ)

Vol.20, No.1, 2024 *p 21 – 42*

PALEOSTRESS ANALYSIS USING FRACTURE DATA, A CASE STUDY OF KEWA CHARMULA ANTICLINE, KURDISTAN REGION, NORTHEASTERN IRAQ

Jihad H. Majeed[1*] and Salim H. Sulaiman Al-Hakari[2]

[1] Assistant Lecturer; Department of Geology, College of Science, University of Sulaimani,
[*]Correspondence e-mail: jihad.majeed@univsul.edu.iq; Jihad H. Majeed
[2] Assistant Prof. Dr. Department of Geology, College of Science, University of Sulaimani.

Type of the Paper: Article
Received: 04/ 11/ 2022
Accepted: 05/ 02/ 2023

Keywords: Kewa Charmula; Kirkuk Fault; Stress Permutation; Low Folded Zone; Zagros Fold-Thrust Belt.

ABSTRACT

Fracture analysis was carried out through three adjacent traverses. The study area is considered a part of the Arabian Plate and geologically falls within the boundary between the Low Folded Zone and the High Folded Zone of the Western Zagros Fold-Thrust Belt in the Iraqi Kurdistan Region. Five formations are cropped out in this anticline, extending from the Late Oligocene up to the Late Miocene – Pliocene. Those formations are (Anah, Jeribe, Fatha, Injana, and Mukdadiya). In addition, identify an Oligocene unit the Kirkuk Group, represented by the (Anah Fn.) that no other studies have previously referred to, in addition, to observing the Jeribe Formation along Tilyan Gorge. About 350 fracture planes were measured for the study and classified into sets and systems concerning their relations to the three mutually perpendicular geometrical axes (tectonic axes). Tension sets are (ac), which are formed by extension along the fold axis accompanying direct compression perpendicular to the fold trend, whereas the (bc) set is supposed to be the product of relaxation that motivated the primary compressional stress. The shear systems are each of hk0, h0l, and 0kl developed successively during direct compression and subsequent relaxation episodes of each tectonic stress. The results of the paleostress analyses showed that there is a general coincidence in the direction of the major stress axis (σ1) and the minor stress axis (σ3), which were derived from the joints (fracture planes). Joints are presented as sets and systems. The analysis of joint attitudes revealed that the joints might be due to the influence of the main horizontal compression paleostress in the direction NE – SW that is responsible for folding, or they might be caused by the stretching of the outer arc for the folded layers. According to field observations and paleostress studies, the region experienced four stress stages. The first is a main compressive tectonic phase in the NE – SW direction. The second phase is the second compressive tectonic stress in the direction NW – SE. The third was a NE – SW extension tectonic phase that originated during the final uplift stage of folding and it is representative of the major fold trend. The fourth is the NW – SE extension face considered as the extension stress connected to the principal NE – SW compressive stress.

1. INTRODUCTION

The study area, which is located in the Iraqi Kurdistan Region, is regarded to be a part of the Arabian plate while, geologically, falls within the boundary between the Low Folded Zone and the High Folded Zone of the Western Zagros Fold-Thrust Belt. The anticline chosen for the study is 9.5 Km in length and about 2.8 Km in width, with an NW – SE trend, called the Kewa Charmula anticline, with no previously published geological study on it, except for oil company studies that are confidential. The study area is located in the eastern part of the northwestern segment of the Zagros Fold-Thrust Belt (ZFTB) in (the Sulaimani Governorate), Iraqi Kurdistan region, at the northeastern margin of the Arabian plate. The area lies in between longitudes (44°52' – 44°46' E) and latitudes (35°42' – 35°46' N), it occupies around 36 Km^2 in the Iraqi Kurdistan Region (Figure 1). The Kewa Charmula anticline is located in the center of the area. Geographically is located about 58 Km southwest of Sulaimani city, and 48 Km NE of Kirkuk city, also about 7 Km SW of Aghjalar town, additionally the anticline makes an echelon relation with its neighbor Qishlakh anticline at SE, is also surrounded by several local villages which are (Tawakall at E, Kani Anjir at NE, Tilyan and Tizha at SW and Kani Araban at S).

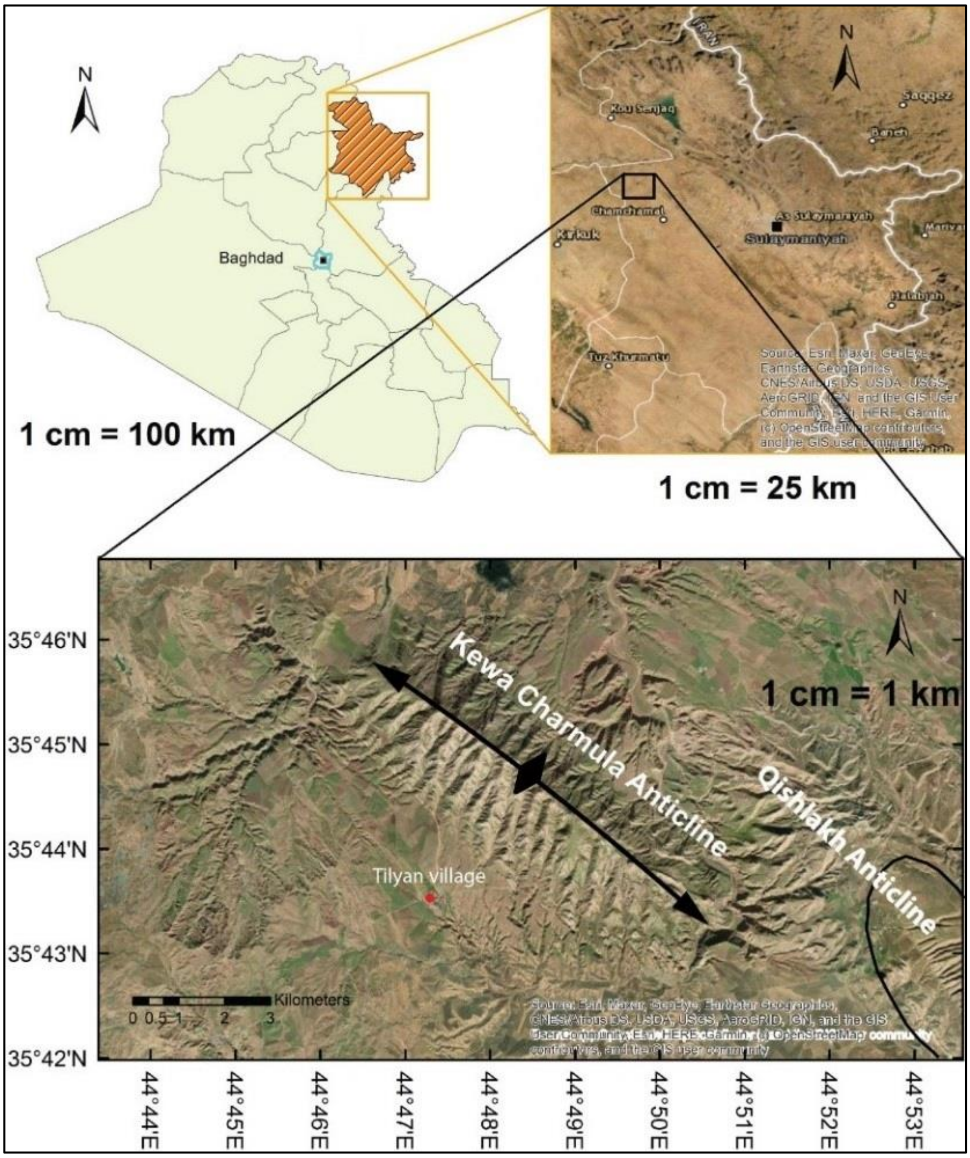

Figure 1: Location map of the study area.

2. TECTONIC OF THE STUDY AREA

The studied area, which is considered to be the northeastern part of Iraq, is located on the northeastern boundary of the Arabian Plate. The NW – SE trending Najd rifting event (610 – 520) Mega Annum (MA), which began in the Late Precambrian, generated the NW – SE trending Najd fault system in Iraq, which is prominent in the basement of northern Iraq and impacts the margins of tectonic zones (Jassim & Goff, 2006). The Arabian Plate was exposed to crustal expansion (rifting) throughout the Permian, resulting in the separation of the Iranian Terranes and the spread of the Neo-Tethys Ocean. From the late Permian to the Cretaceous, the region became a post-rift passive margin to the southwest of the Neo-Tethys Ocean (Sharland et al., 2001).

Zagros Fold and Thrust Belts (ZFTB) was a final result of the subduction and subsequent collision between the Arabian and Eurasian plates. The orogeny began in the Late Cretaceous with ophiolite obduction on the Arabian Plate border (Ghasemi & Talbot, 2006). The continental collision began in the Miocene along the orogeny's southeastern section and the Oligocene belongs to the northwestern part of the orogeny. The impact caused the Neo-Tethys Ocean to close (Blanc et al., 2003).

The Zagros Mountains in northeastern Iraq and southwestern Iran are part of the Alpine Himalayan Mountain range. They are bounded to the NE by the Central Iranian Plateau, to the NW by the Taurus Mountains in Turkey, and to the SE by the Oman Fault (Talbot & Alavi, 1996).

Most of the recent descriptions of the Zagros Orogeny use some modification of the structural zones proposed by Falcon (1969). The study area is located at the boundary between the High Folded Zone and the Foothill (Low Folded) Zone. These zones are identified on the basis of abrupt geomorphic changes often corresponding to major surface faults. Kent (2010). The Zagros Orogeny is subdivided into four NW – SE striking tectonic units in the Kurdistan Region of Iraq: The Zagros Suture, the Imbricated Zones, the High Folded Zone (similar to the Simply Folded Belt in the Iranian side of the Zagros), and lastly the Foothill (Low Folded) Zone (Jassim & Goff, 2006) and (Fouad, 2015) shown in Figure (2). The study area is located at the boundary between the High Folded Zone and Foothill (Low Folded) Zone, regarding the mentioned classification.

3. STRATIGRAPHY

The stratigraphic successions of the studied area have been dominated by the exposures of rock units ranging from Late Oligocene (represented by Anah Fn.), then Middle Miocene (Jeribe Fn.) to Late Miocene-Pliocene (Bakhtiari Group).

In the meantime, we are the first to identify an Oligocene unit the Kirkuk Group, represented in that region by the (Anah Fn.) that no other studies have previously referred to (Figure 3). The Anah Formation was merely found along Traverse #2 (Figures 4 & 5), with no evidence for its existence along all three other Traverses (Figure 6). During the Miocene period, the region to the west of the Zagros Mountain Front Fault (ZMFF) subsided under the load of the elevated units forming the Tertiary foreland basin (Figure 9).

Moreover, In the Tertiary foreland basins, the Miocene-Pliocene formations (Jeribe, Fatha, Injana, and Mukdadiya) were deposited. As a result, during the Oligocene, a continental collision between the Arabian and Eurasian plates caused the rising of the areas of the region, the area is located between the Zagros Mountain Front Fault (Figure 10) and the Kirkuk Fault in the (Chemchamal-Butmah Subzone), which was a high land area in the Oligocene; therefore, the Oligocene units were not deposited. Resulting in the extinction of Oligocene rock groups

(Ameen & Othman, 2012; Ibrahim, 2009). The previous units were overlain by thick evaporates, carbonate, and marls of the Fatha Formation during the Middle Miocene, resulting from shallow water carbonates flowing up into evaporates (Jassim & Goff, 2006).

After a brief period of marine sedimentation following the deposition of evaporitic Fatha Formation, (Figure 7), clastics from the rising orogen in the north reached the basin in vast quantities around the beginning of the Upper Miocene. These clastics are deltaic-sedimentary and begin with red silts and marls Injana Fn. (Dunnington, 1958).

Then the Injana Fn. overlaid by the Mukdadiya Fn., (Figure 8), which was deposited in a rapidly subsiding foredeep basin in a fluvial environment (Jassim & Goff, 2006). Regionally, the formation is connected with transitions and gradual changes in the character of the sedimentation with the Injana Formation. In the study area, the first appearance starts with the bed of Pebbly Sandstone which indicates shallowing in the sedimentary basin.

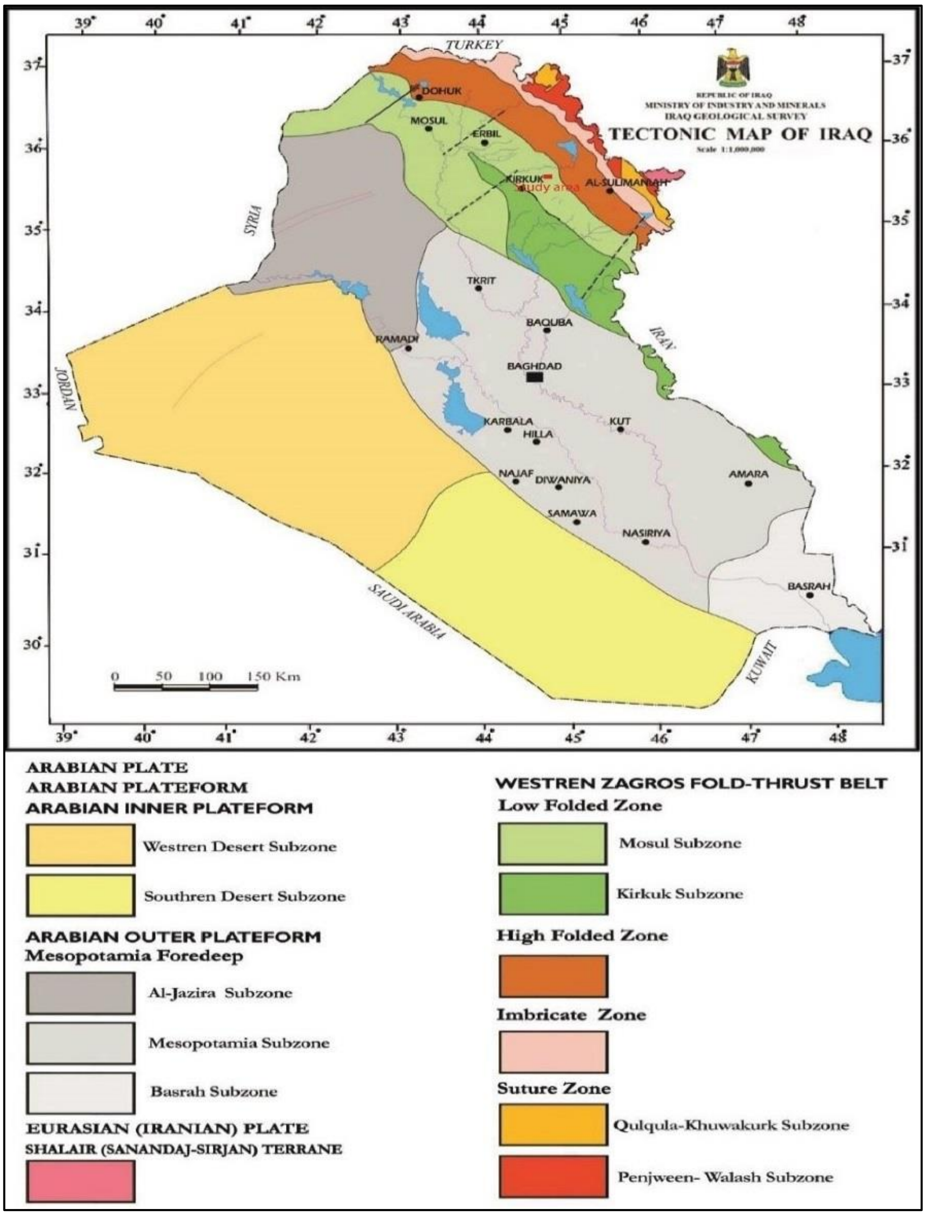

Figure 2: Tectonic divisions of northern Iraq (compiled Fouad, 2015).

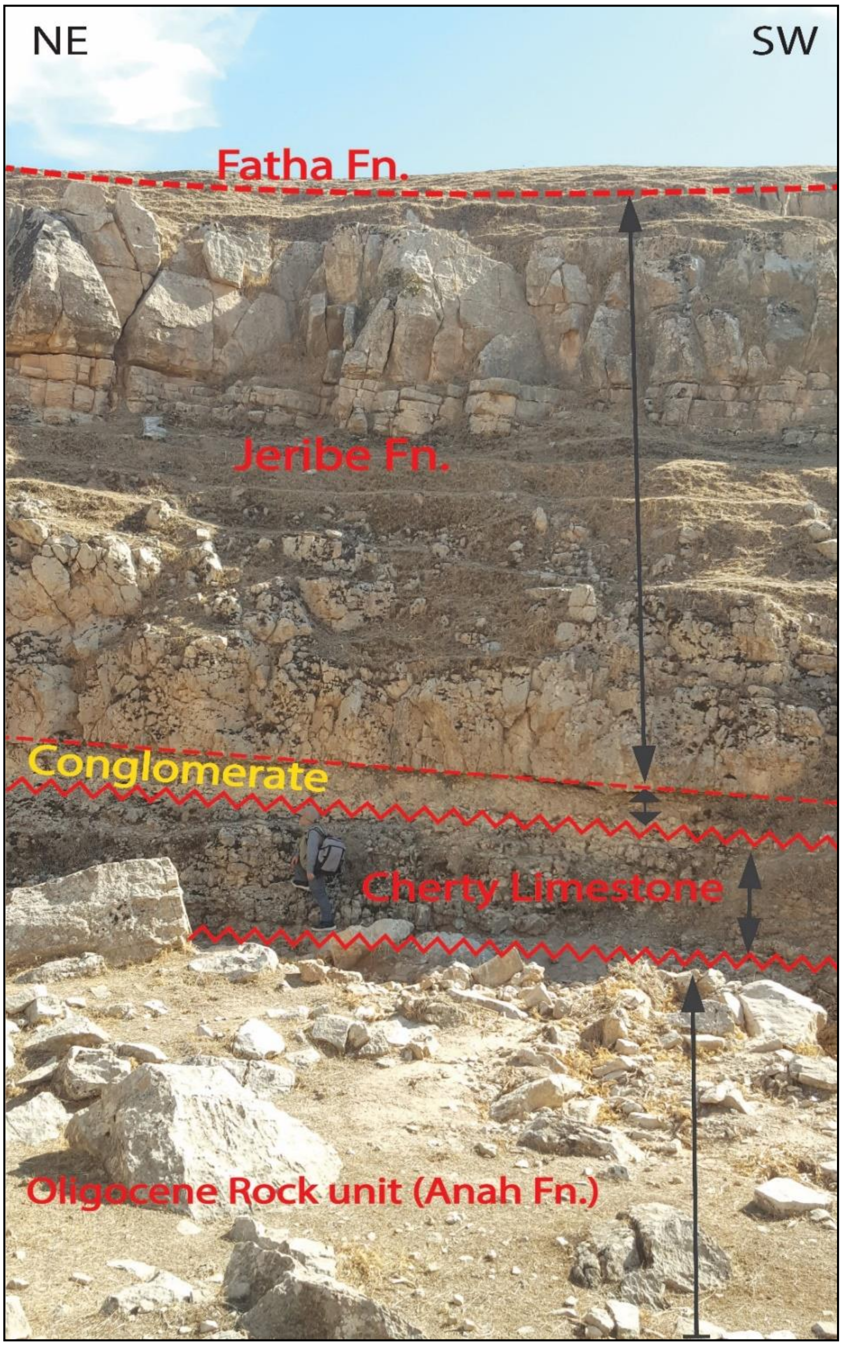

Figure 3: Exposing Anah and Jeribe formations beneath Fatha Fn.; Tilyan Gorge, Traverse #2, southwestern limb (SWL).

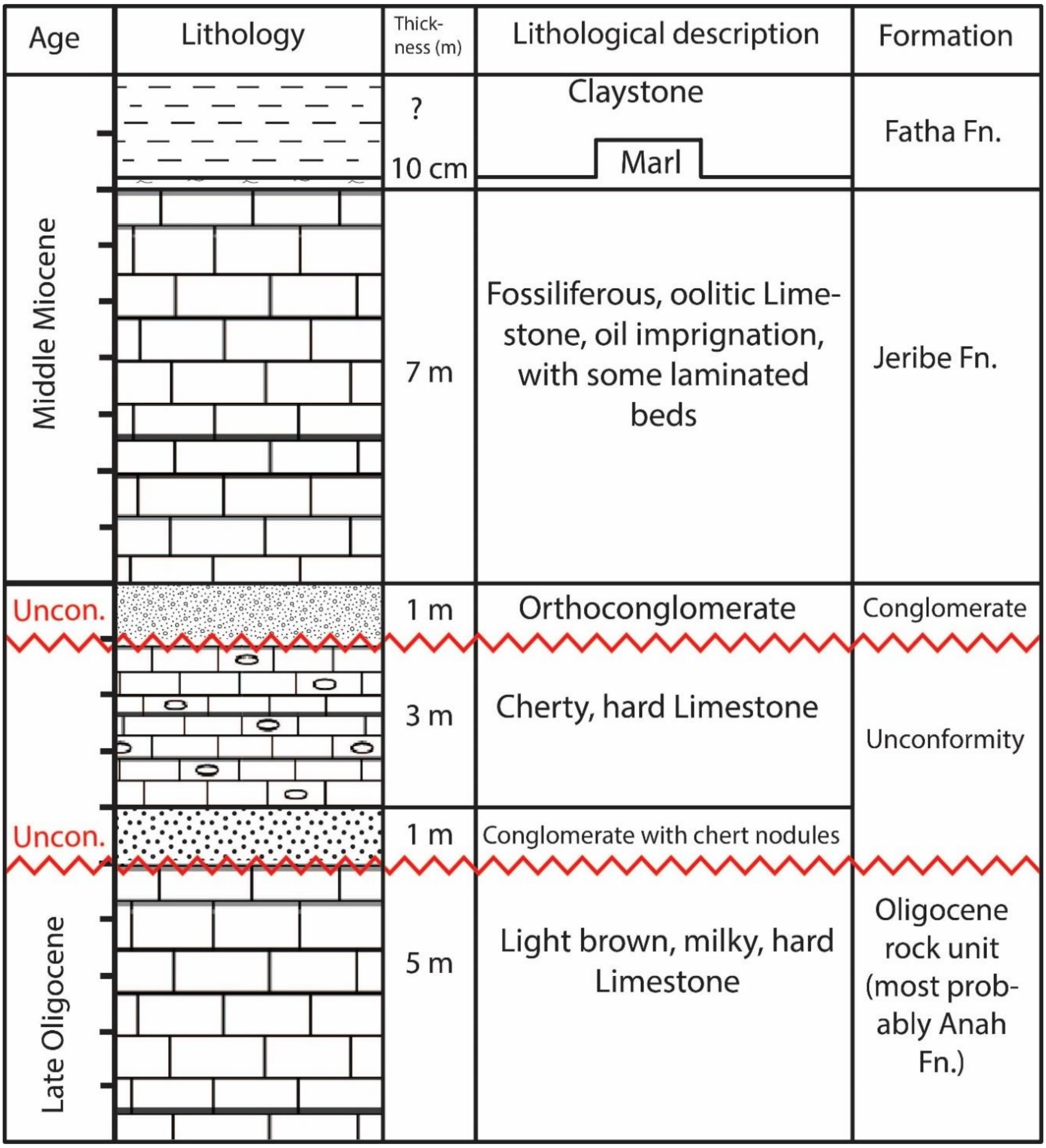

Figure 4: Illustrates the columnar section of the Tilyan gorge, along Traverse #2, the southwestern limb (SWL).

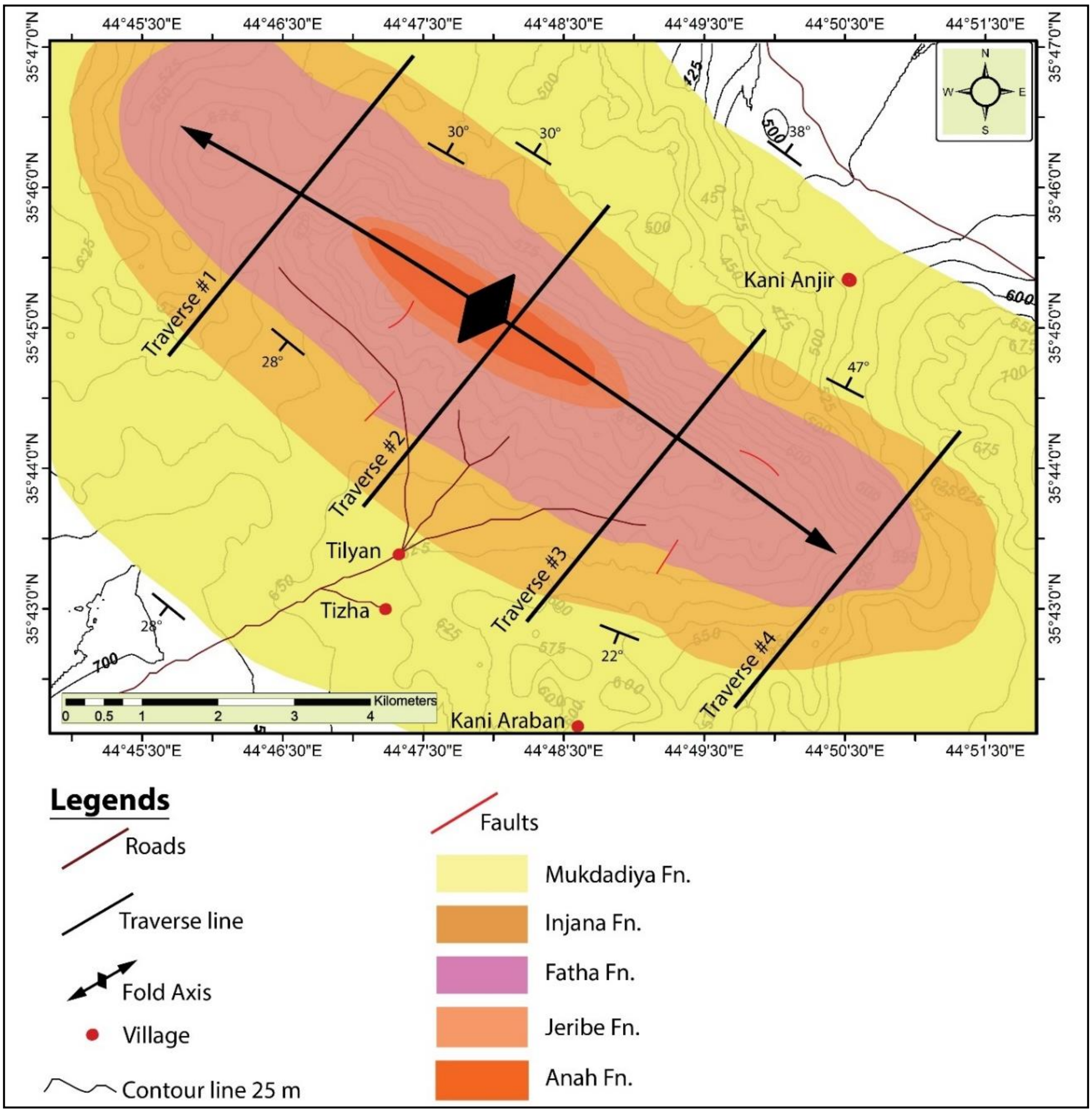

Figure 5: Geological map of the study area, showing all four mentioned traverses.

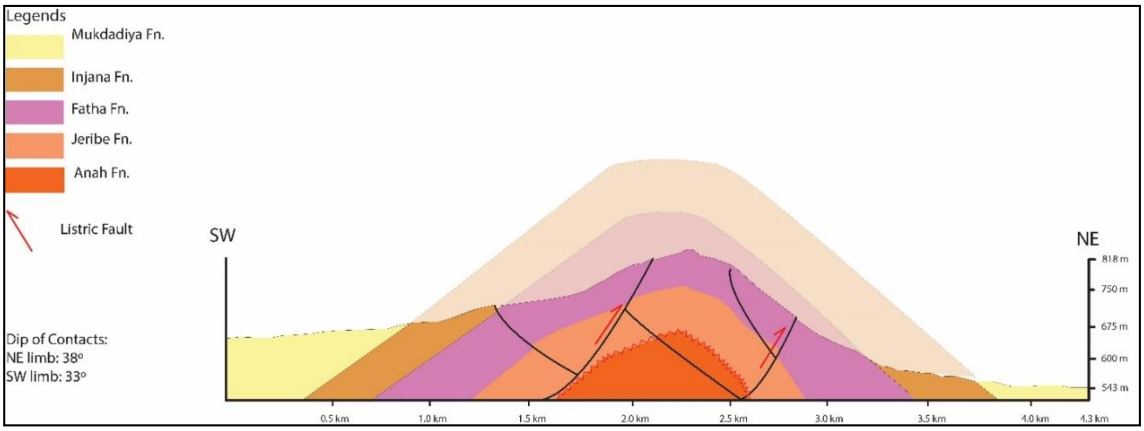

Figure 6: Geological cross-section along Traverse #2, showing different formations.

Figure 7: Field photo of the Gypsum bed of Fatha Fn. in the outcrop.

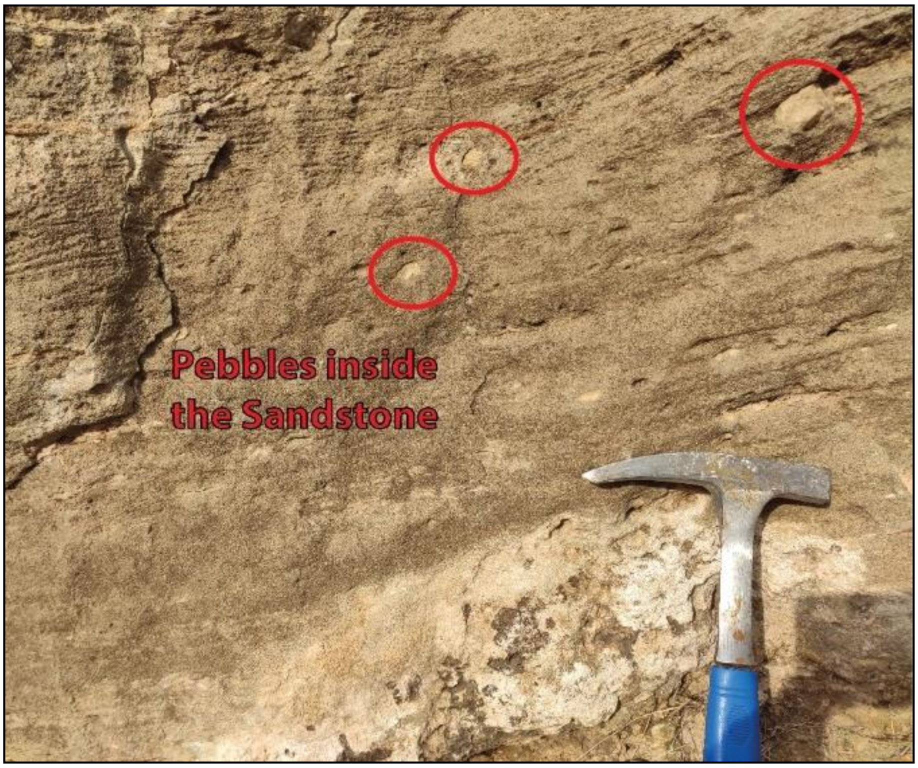

Figure 8: First appearance of the pebbly sandstone of the Mukdadiya Fn. in the field, Traverse #2, NEL.

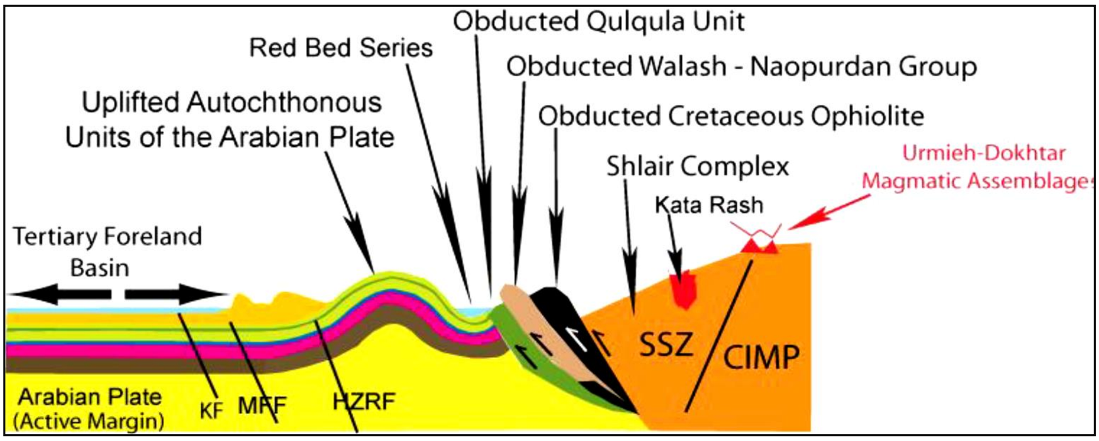

Figure 9: Tectonic setting of the Arabian Platform (including the study area) in Miocene and onwards. The Tertiary foreland basin was formed under the load of the elevated units (after Ibrahim, 2009).

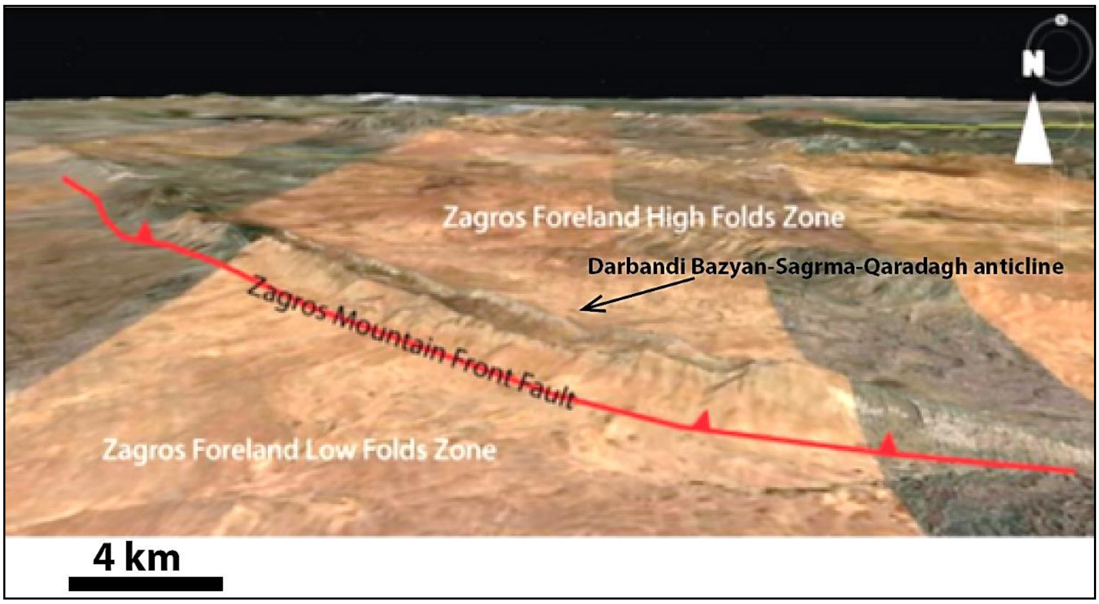

Figure 10: Google Earth image of a sudden change in topography over the Zagros Mountain Front Fault (ZMFF), the Darbandi Bazyan-Sagrma-Qaradagh anticline series separates the Zagros High Folds Zone from Zagros Low Folds Zone (after Ibrahim, 2009).

Fractures are one of the most prevalent geologic phenomena. Their study is beneficial because they yield information about the history of deformation. A fracture is a planar or sub-planar discontinuity that arises as a result of external (tectonic) or internal (thermal or residual) forces (Fossen, 2010). Fractures are classified as shear fractures (slip surfaces), opening fractures (joints), fissures, and veins; some geologists also include compaction fractures or anti-cracks (stylolite) (Fossen, 2010).

An increase in the quantity and variety of joints is typically associated with the production of tectonic folds and faults in the brittle crust (Brittle Deformation). The fact that certain joint sets before the faulting or folding, while others followed or evolved after the structures were established, makes it difficult to investigate these fracture systems (Mandl, 2005).

4. JOINTS

Joints are the most widespread geological structures that have formed in the upper crust (Weinberger et al., 2010). A joint is a natural fracture in a rock that has not been sheared (Billings, 1972; Bles & Feuga, 1986; Fossen, 2010; Hancock, 1985; Ramsay & Huber, 1987; van der Pluijm & Marshak, 2004).

The physical properties of joints as well as the information they provide about the sequence of tectonic events responsible for their formation are crucial for understanding rock evolution. Tension joints are usually accepted to form a mode of fracture parallel to the maximum compressive principal stress axis and perpendicular to the minimum principal stress axis (the direction in which the rock is stretched) (Engelder & Geiser, 1980). Many joint investigations have been conducted to determine the direction of the stresses that the rocks have been exposed to (Billings, 1972).

5. DATA AND METHODS

The fieldwork was carried out to obtain measurements of fracture planes through 18 stations distributed in the study area along the three adjacent traverses (#1, #2, and #3). The stations were selected far from the plunging area to avoid the tectonic axes rotation and give the most accurate and realistic results (Figures 18, 19, and 20). All measurements and results are in the Right Hand Rule (RHR). The measurements from the field included the attitudes of bedding and fracture planes.

The fracture plane data were analyzed stereographically using Dips software (v.6.0). The results of fracture plane analysis were classified and compared according to Hancock & Atiya (1979).

GeoCalculator software (v.4.9.8) is used to determine the paleostress directions of each ($\sigma1$, $\sigma2$, and $\sigma3$) from the average attitudes of the conjugate shear fracture planes. $\sigma1$ bisects the acute angle between conjugate shear fracture planes, $\sigma3$ is perpendicular to $\sigma1$ and bisects the obtuse angle, and $\sigma2$ represents the line of the intersection between the two fracture planes (Anderson, 1942). The tension fractures are usually perpendicular to the least principal stress ($\sigma3$) and parallel to the maximum stress direction ($\sigma1$). Finally, the resulting output of the geometrical analyses of structural mode (fractures) was unified and arranged to conclude the sequence of tectonic phases, which modified the study area regarding the geotectonic setting of the studied area (Figure 23).

6. RESULTS

6.1. The Geometry of the Fold

The Kewa Charmula anticline was studied geometrically through four traverses that were perpendicular to its axis. The study along these traverses revealed that the anticline follows the same general Zagros fold trend (NW – SE), and the anticline is considered asymmetrical, cylindrical, or sub-cylindrical in general, while along Traverse #2 (for instance), the fold is rather considered as cylindrical (see Figure 16), double plunge box fold along Traverse #2 (Figure 13). It consists of a crestal segment bounded by two limbs (Figure 15). The southwestern limb is slightly steeper than the northeastern limb. The (Figure 11) shows the synoptic Equal area stereographic pi-diagram of the Kewa Charmula anticline along (Traverse #2). The average

attitude for the southwestern limb is 145/33°, while the northeastern limb is 303/38°, the interlimb angle is 70° and the anticline is (Close) according to the classification by van der

Pluijm & Marshak (2004). The Axial Plane is 135/87° whereas the Fold Axis is 314/10°, (Figure 17) and the fold orientation is Horizontal Upright (Figure 12) according to Fleuty (1964).

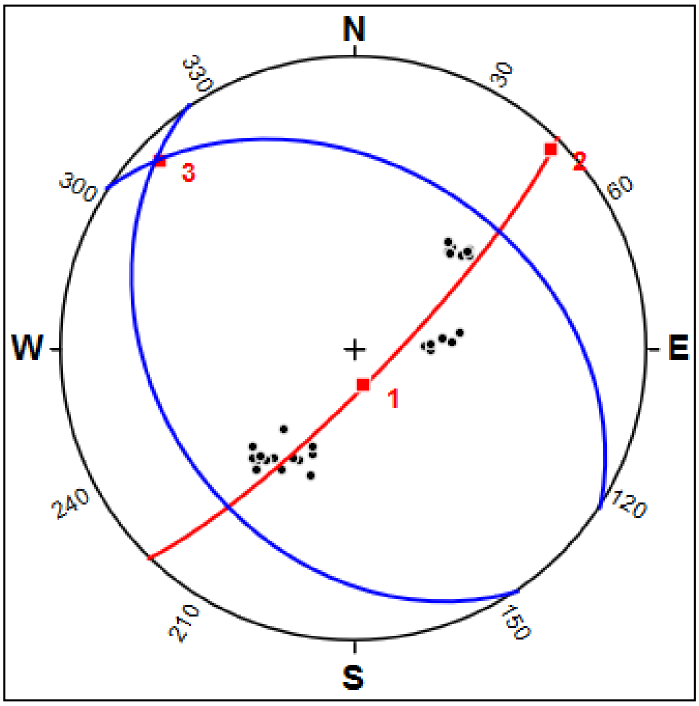

Figure 11: Synoptic pi-diagram of the Kewa Charmula anticline along cross-section (Traverse#2).

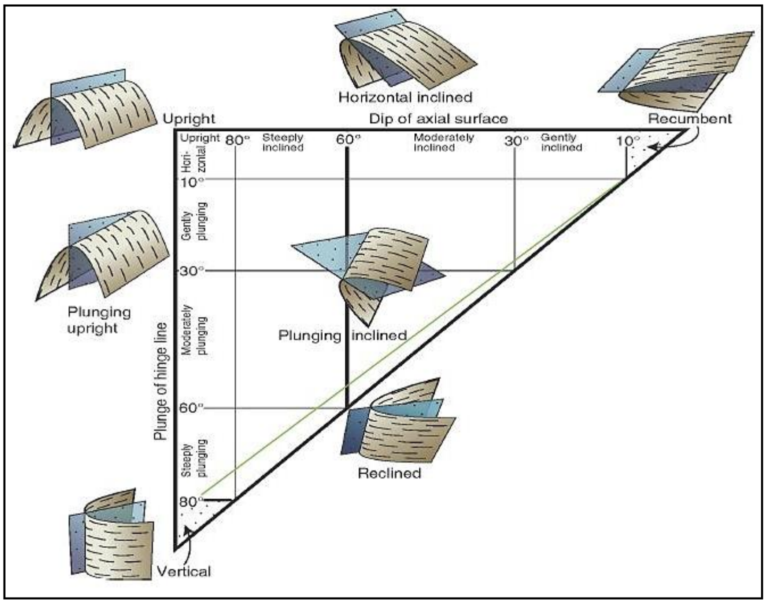

Figure 12: Fleuty (1964) fold classification of fold (Fossen, 2010).

6.2. Fracture analysis

More than 350 fracture planes data points were gathered from 18 different locations across three traverses (Figure 13), while the last station (station number 19) was neglected due to the intensity of deformation along the SE plunge. The strike and dip of fracture planes were measured and documented in each station, as well as the attitude of the bedding plane, which contained the fractures. Much of the collected data was neglected due to the lack of the two conjugate fractures of the system in the same station. The stereographic projections of the fracture poles in each of the 18 locations are presented in (Figures 18, 19, and 20). Table 1 lists all data with a paleostress categorization.

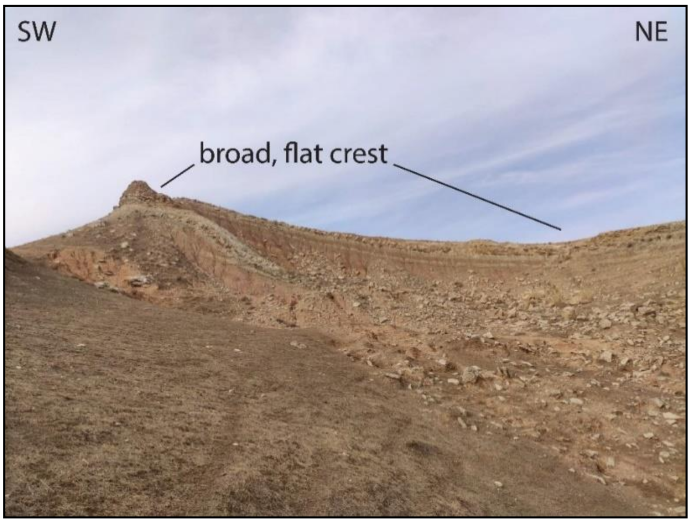

Figure 13: Clarifies that the crest of the fold is broad and flat along Traverse #2.

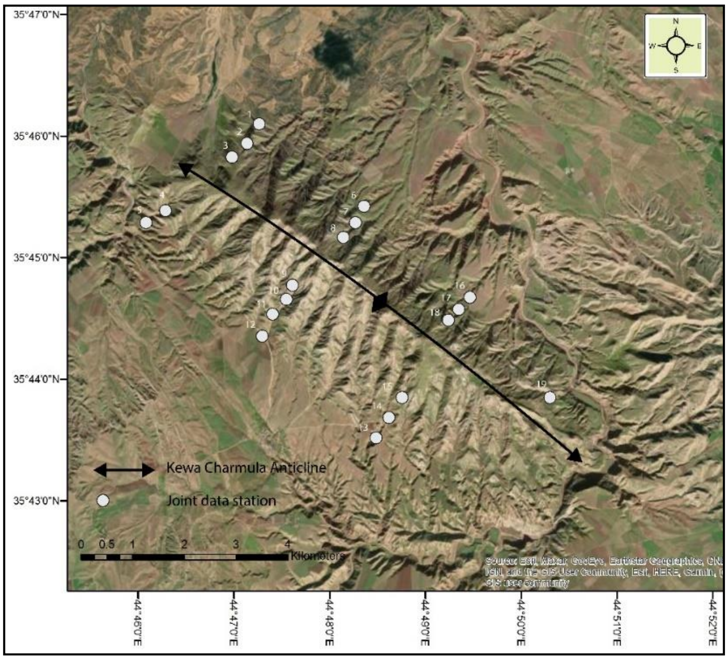

Figure 14: Location of (19) joint data stations along the study area.

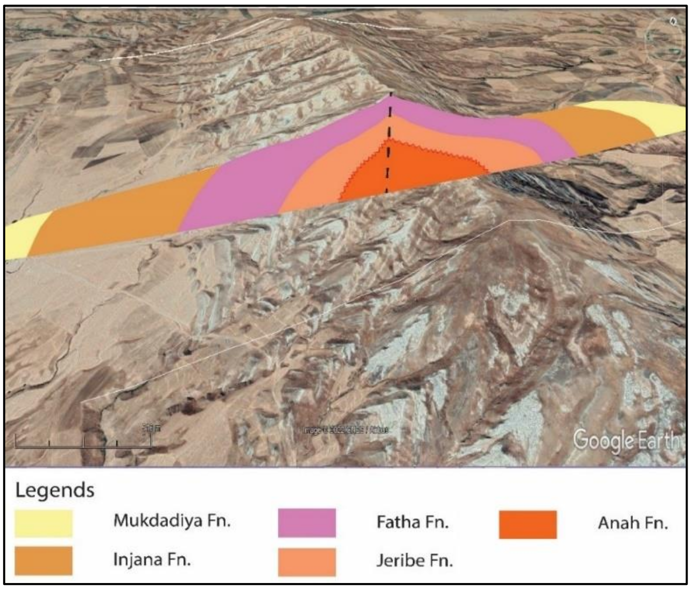

Figure 15: Cross-sectional view of Traverse #2 (Tilyan Gorge), showing exposed formations, Anah and Jeribe formations were studied for the first time (photo extracted from Google Earth).

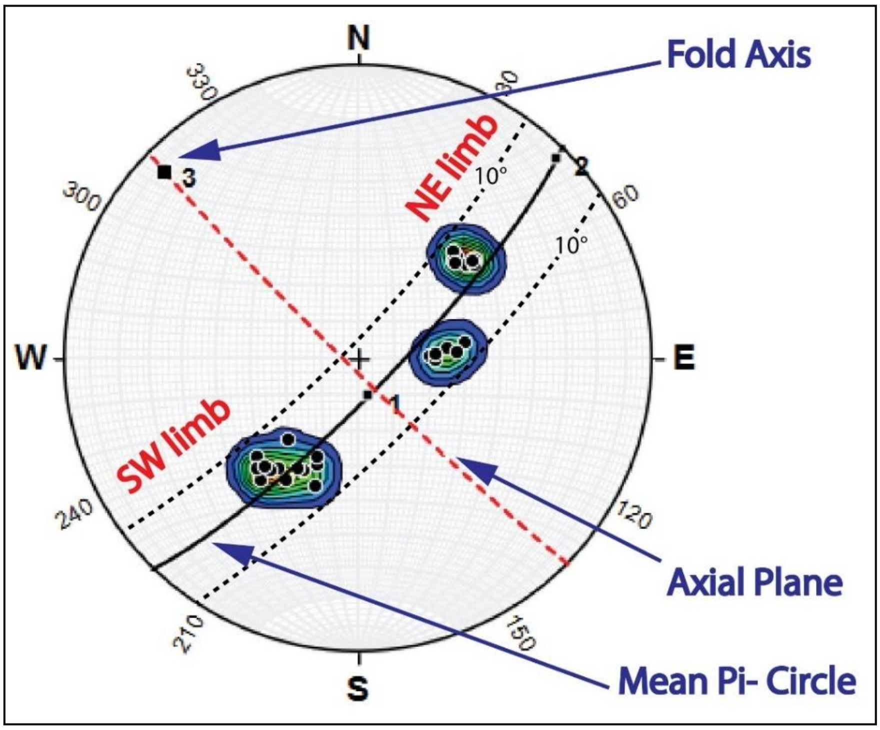

Figure 16: Illustrates Pi-diagram for pole projection of Traverse#2 along Kewa Charmula anticline, to obtain the cylindricity of the fold, which is classified according to (Ramsay & Huber, 1987).

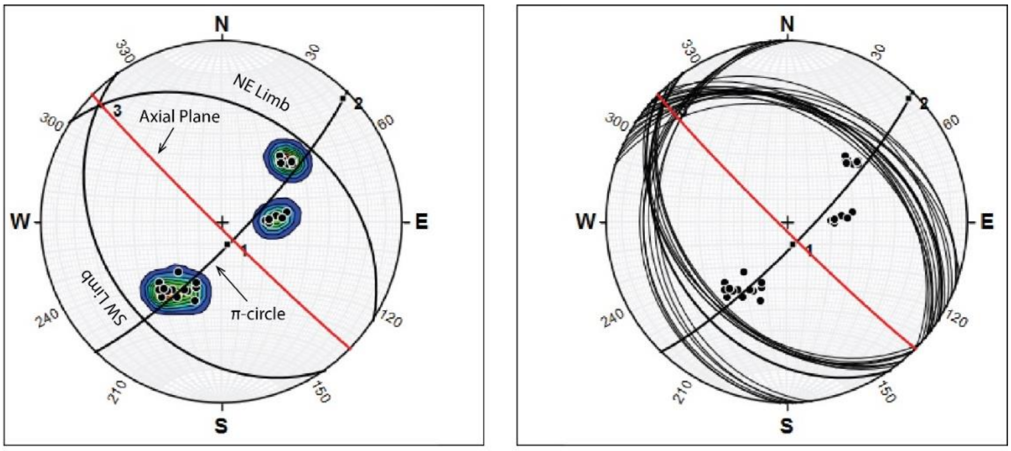

Traverse #2
Axial Plane: 135/87
Fold axis: 314/10 (trend/plunge)
π-circle (best fit great circle): 044/81
Interlimb angle: 70°
Average attitude for SW Limb: 145/33
Average attitude for NE Limb: 303/38

Figure 17: Shows Pi-diagram for entire bedding planes along Traverse #2.

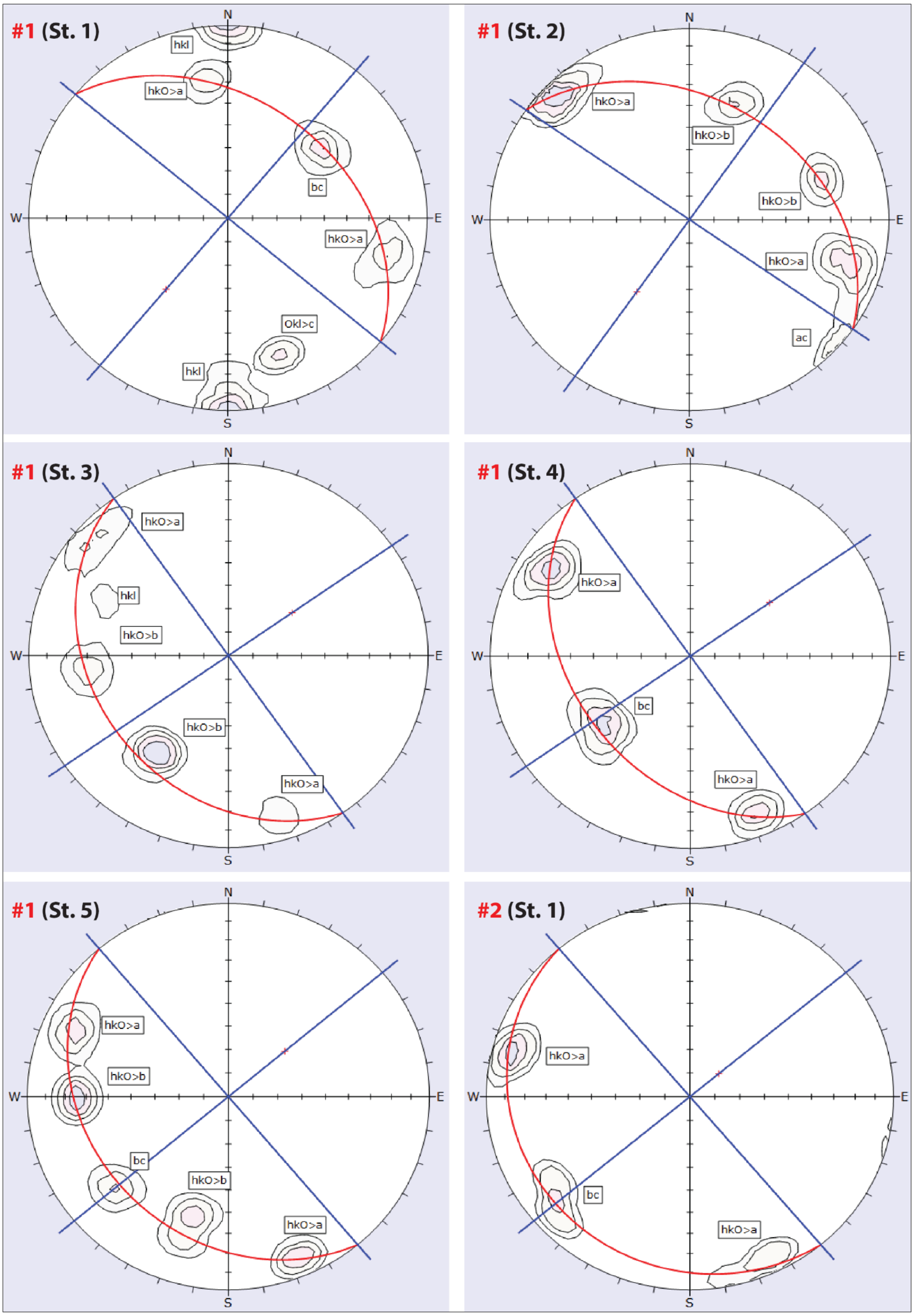

Figure 18: Pole projections (fractures) and classification for the stations along Traverses (#1 & #2).

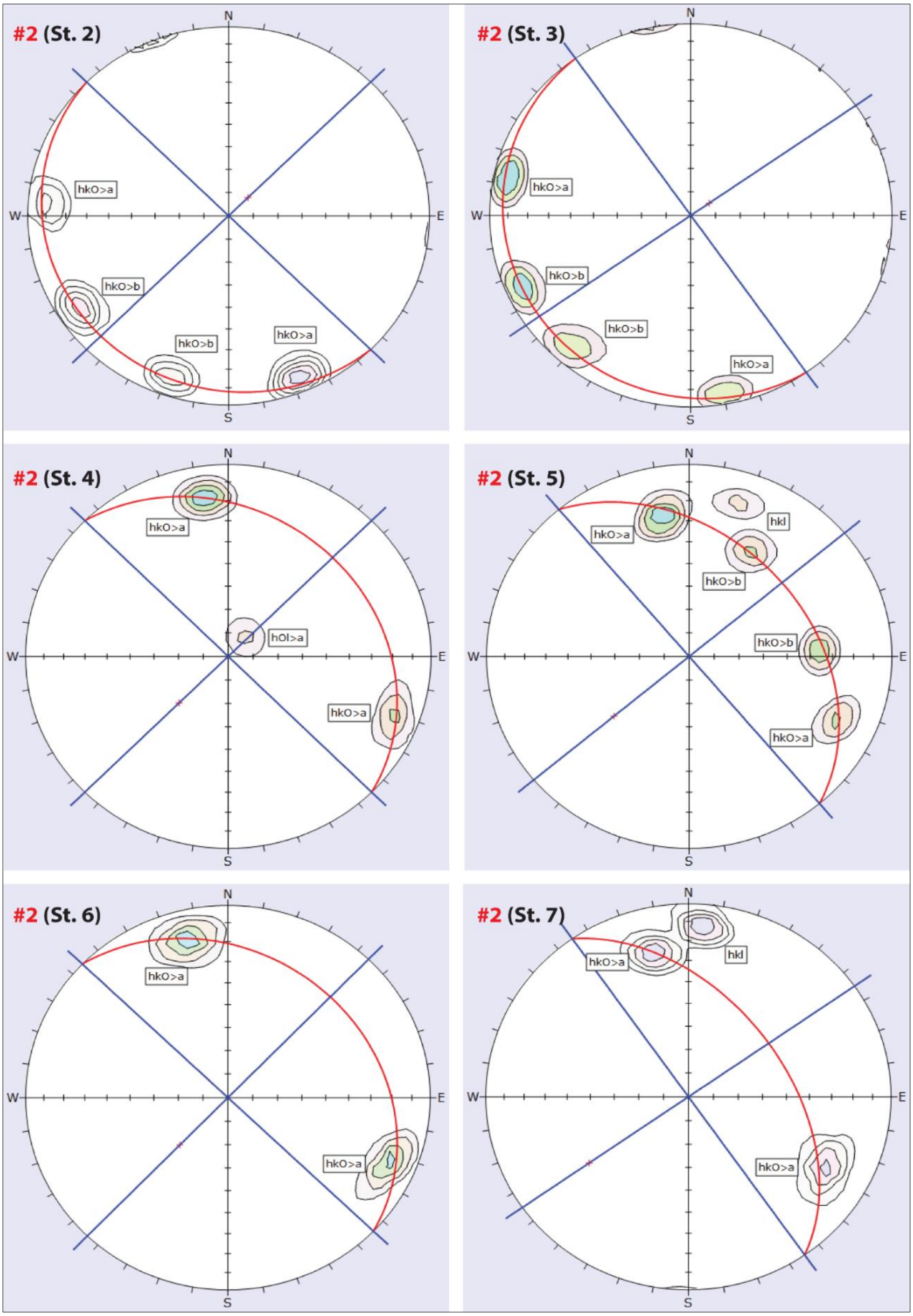

Figure 19: Continued, pole projections (fractures) and classification for the stations along Traverse #2.

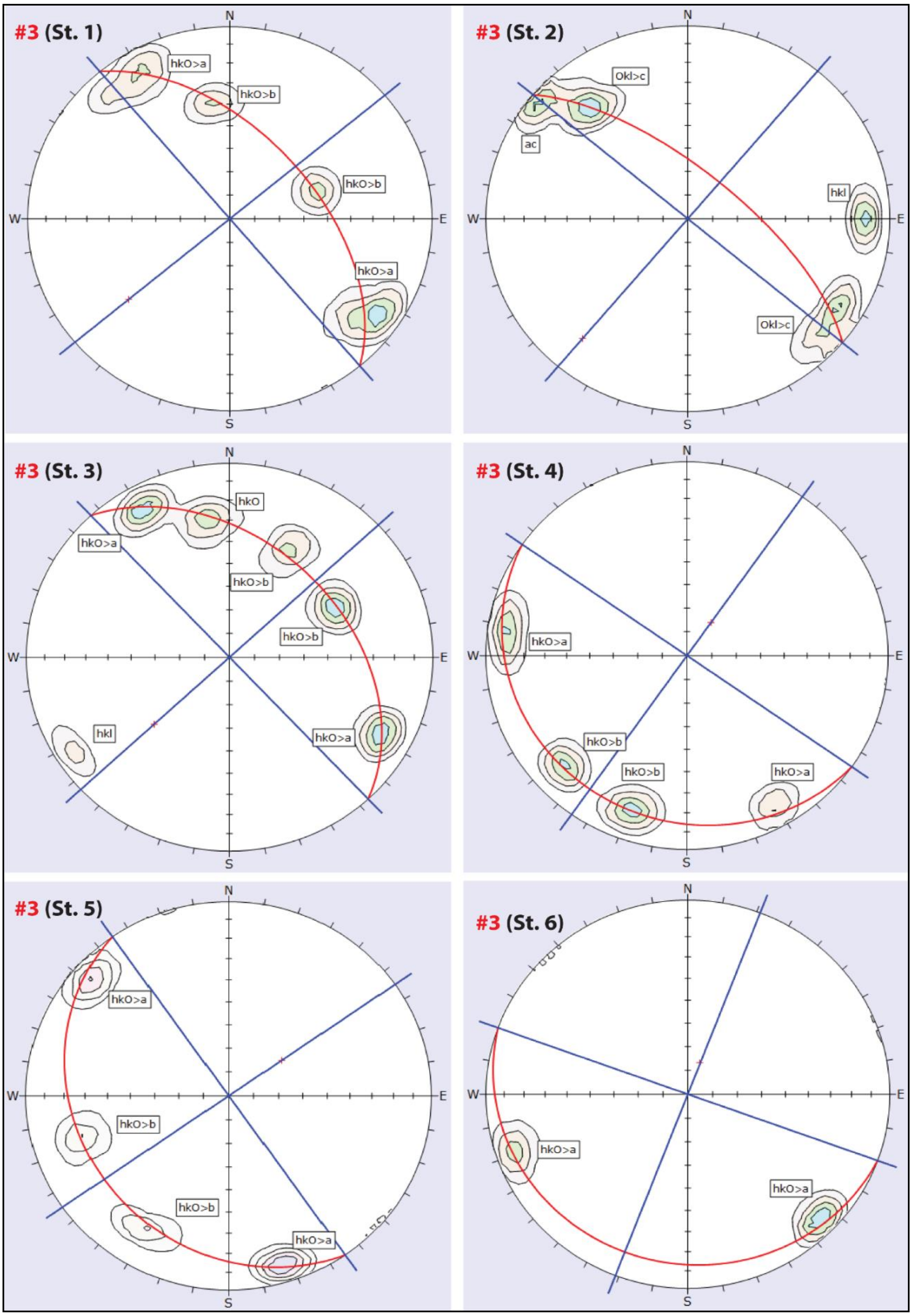

Figure 20: Continued, pole projections (fractures) and classification for the stations along Traverse #3.

Table 1: Fracture types and paleostress analysis for all 18 stations three traverses (#1, #2, and #3) in the study area.

Traverse	Station	Bedding plane	Type of Fracture	Average attitude of the conjugate fracture planes		Paleostress analysis Plunge/Trend			Stress direction	Type of applied Stress
						σ1	σ2	σ3		
#1	1	130/40	bc	321/50	--	00/000	00/000	00/000	NE-SW	Tension
			hkO>a	261/61	014/70	40/231	50/040	05/136	NE-SW	Compression
			Ok1>c	197/63	070/64	48/043	42/224	01/134	NE-SW	Tension
	2	125/38	ac	038/88	--	00/000	00/000	00/000	NW-SE	Tension
			hkO>a	224/82	014/74	39/206	50/034	04/299	NE-SW	Compression
			hkO>b	288/53	342/58	05/132	52/035	38/226	NW-SE	Compression
	3	325/32	hkO>a	221/81	073/77	35/058	55/234	02/327	NE-SW	Compression
			hkO>b	174/60	126/55	06/326	54/228	35/061	NW-SE	Compression
	4	325/40	bc	140/47	--	00/000	00/000	00/000	NE-SW	Tension
			hkO>a	213/72	068/78	42/048	48/234	03/141	NE-SW	Compression
	5	320/30	bc	140/62	--	00/000	00/000	00/000	NE-SW	Tension
			hkO>a	204/75	067/80	31/044	59/230	03/136	NE-SW	Compression
			hkO>b	179/65	107/60	04/321	57/225	33/054	NW-SE	Compression
#2	1	320/15	bc	140/74	--	00/000	00/000	00/000	NE-SW	Tension
			hkO>a	196/81	066/83	18/041	72/224	01/131	NE-SW	Compression
	2	315/11	hkO>a	186/82	066/82	15/036	74/218	00/126	NE-SW	Compression
			hkO>b	147/77	109/79	03/129	78/218	13/038	NW-SE	Compression
	3	325/09	hkO>a	193/81	079/85	13/046	77/237	02/136	NE-SW	Compression
			hkO>b	156/80	132/81	02/144	80/248	10/054	NW-SE	Compression
	4	135/28	hkO>a	261/73	020/77	28/231	62/046	02/140	NE-SW	Compression
			hO1>a	312/11	--	00/000	00/000	00/000	NE-SW	Compression
	5	140/40	hkO>a	260/65	024/69	42/234	48/049	02/142	NE-SW	Compression
			hkO>b	355/55	298/52	03/144	50/051	40/237	NW-SE	Compression
	6	134/28	hkO>a	256/73	021/76	31/229	59/045	02/138	NE-SW	Compression
	7	145/50	hkO>a	256/65	030/63	51/232	39/054	01/323	NE-SW	Compression
#3	1	140/55	hkO>a	239/77	036/73	53/225	37/049	02/318	NE-SW	Compression
			hkO>b	340/37	263/52	12/311	35/050	52/205	NW-SE	Compression
	2	130/70	ac	219/86	--	00/000	00/000	00/000	NW-SE	Tension
			Ok1>c	230/64	034/74	61/008	19/240	21/142	NE-SW	Tension
	3	137/42	hkO>a	241/77	028/73	43/223	47/047	02/315	NE-SW	Compression
			hkO>b	333/48	295/50	03/317	47/050	43/224	NW-SE	Compression
	4	305/17	hkO>a	187/81	061/78	22/035	68/210	02/304	NE-SW	Compression
			hkO>b	137/71	109/72	02/124	71/220	19/033	NW-SE	Compression
	5	325/26	hkO>a	221/82	073/78	33/058	57/234	02/327	NE-SW	Compression
			hkO>b	164/64	120/68	05/144	64/245	26/052	NW-SE	Compression
	6	290/14	hkO>a	161/80	043/83	16/012	74/198	02/102	NE-SW	Compression

7. DISCUSSION

The fracture analysis and classification revealed two orthogonal tension fracture sets (ac) and (bc), as well as the shear systems (hk0) acute about (a), (hk0) acute about (b), h0l acute about (a), h0l acute about (c), and 0kl acute about (c) in the study area. Table 1 demonstrates that the most common paleostress directions are NE – SW, and NW – SE. In the oblique collision of the Arabian and Eurasian plates, a horizontal component of the initial NE – SW compressive stress is considered to be normal to the general trend of the prominent anticline.

This compressive phase resulted in the establishment of (ac) tension, (hk0) acute about (a), and (h0l) acute about (a). The (bc) tension set, and (hk0) acute about (b) show that they were generated by additional compressive stress in the direction NW – SE parallel to sub-parallel to the axes of the major fold. This stress is classified as secondary stress because it originated during the relaxation time following the main compressive stress.

One of the most common shear fractures in the study area is the (hk0) acute about (a) tectonic axis. The shear fractures that are about (h0l) acute about (c) and (0kl) acute about (c) imply that these fractures may be caused by the extensional phase associated with NE – SW and NW – SE compressive stresses (Figure 21).

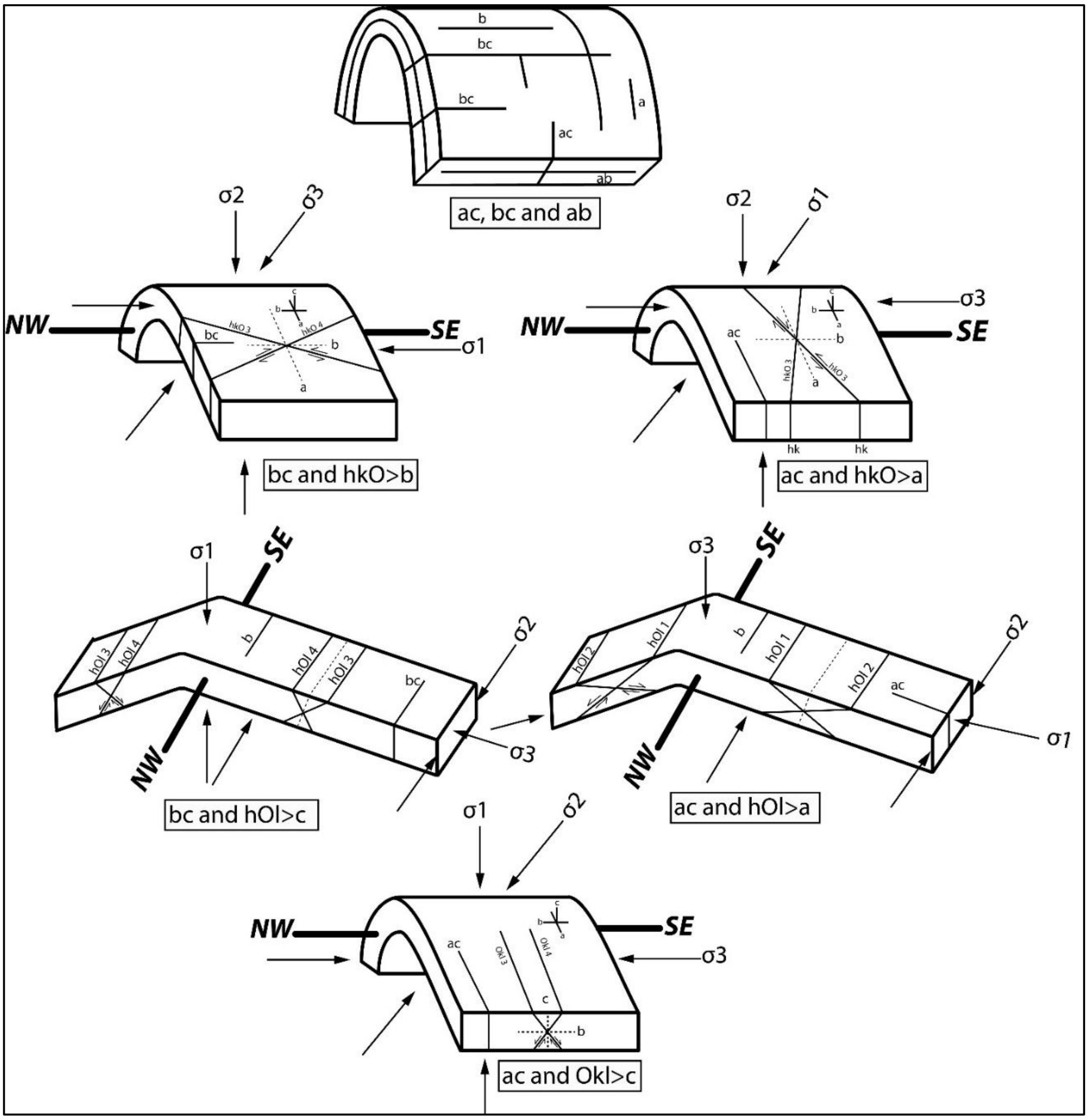

Figure 21: Relation between fracture sets and systems in response to the main stress directions along the Kewa Charmula anticline (according to Hancock, 1985).

The oblique collision of the Arabian and Eurasian plates along their zigzag margins may be responsible for the clockwise rotation of the NNE – SSW paleostress direction to the NE – SW, which is perpendicular to sub-perpendicular to the general trend of the anticline and has maximum stress directions (σ1) (16°/012°) and (42°/234°), respectively (Figure 22).

The anticline formed by the NE – SW stress direction, then developed by the uplifting process that made it to crustal extension, in which the anticline changed from the symmetrical box fold to an asymmetrical NE vergence, which was revealed by the combination of the below fractures, which was analyzed to find the direction of the maximum principal stress ($\sigma 1$).

The primary compressional stress was followed by relaxation, and the (ac) tension joint is the result of such stress. The (bc) is the result of the relaxation that followed the original compression. The extensional phase associated with the NE – SW, and NW – SE compressive stresses led to the development of the corresponding joint system (h0l) acute about (c) and (0kl) acute about (c) shear joints.

Many publications that have researched paleostress in different parts of north and northeast Iraq, such as Taha et al. (1995), Al-Jumaily & Adeeb (2010), and Sulaiman Al-Hakari et al. (2020) have emphasized the two primaries compressional paleostress directions NE – SW and NW – SE, which are also observed as a result of the fracture analysis for the study area.

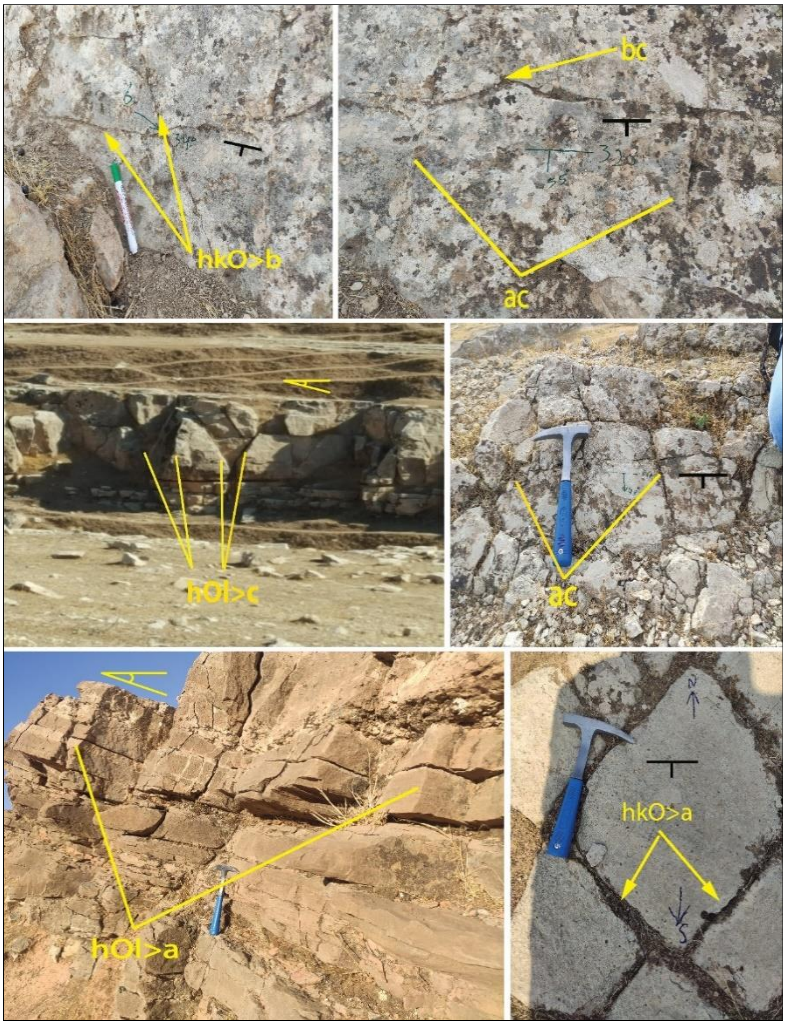

Figure 22: Different types of fractures observed in the study area.

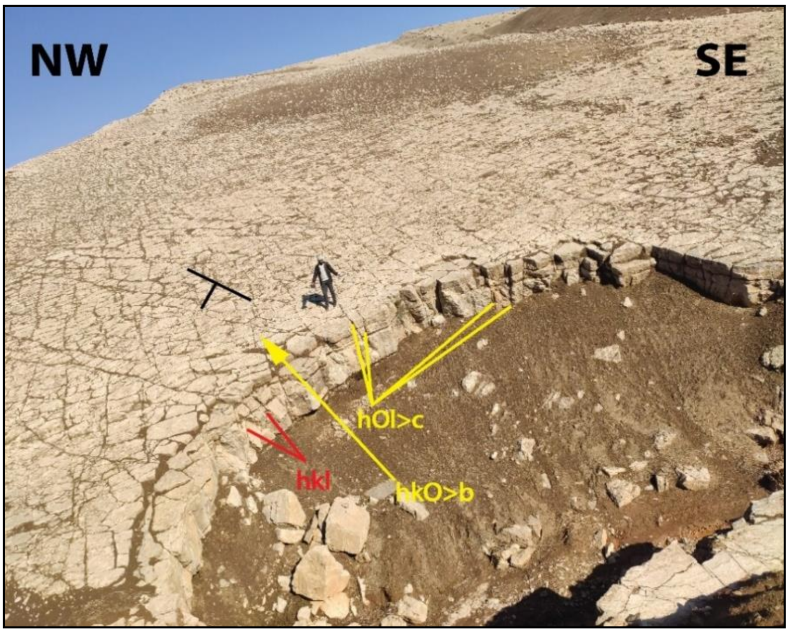

Figure 23: Extensively fractured Limestone bed with different kinds of joint systems along Traverse #4, SWL.

8. CONCLUSIONS

- To be concluded, the paleostress analysis of fractures revealed that the study area experienced the four stress states. Two are compressions, and the other two are extensions.
- The NW – SE compressive stress is parallel to sub-parallel to the fold axis and is regarded as secondary stress that develops during the relaxation event that follows the original compressive pulse. This stress seems to be responsible for the other brittle failures in the region.
- The predominant stress is compressive stress with a maximum horizontal axis (σ1) in the direction of NE – SW, seams being responsible for the initial folding and the majority of the brittle failures in the area.
- The NE – SW extension stress that leads to the NW – SE fractures direction is regarded as a releasing phase, connected with the main final uplift of the fold.
- The NE – SW fracture direction is regarded as an extension stress associated with the main NE – SW compressive stress.
- The clockwise rotation of the NNE – SSW paleostress direction to the NE – SW could be explained by the circumstances of the anticlockwise rotation of the Arabian and oblique collision with Eurasian plates at their zigzag borders.
- The (ac) tension joint sets formed by extension along the fold axis accompanying direct compression perpendicular to the fold trend, while the (bc), is the product of relaxation that succeeded the primary compression. The approximately joint system (h0l) acute about (c) and (0kl) acute about (c) shear joints developed by the extensional phase associated with NE – SW and NW – SE compressive stresses.

REFERENCES

Al-Jumaily, I. S. I., & Adeeb, H. G. M. (2010). Mesofracture Analysis of Azmur Anticline North Eastern Iraq. *Iraqi Journal of Earth Sciences*, *10*(2), 1–24.

Ameen, F., & Othman, P. (2012). New paleoshorelines of the prolific Oligocene/Aquitanian sequence from Zagros fold thrust belt. Kurdistan Region/N. Iraq. *First EAGE Workshop on Iraq-Hydrocarbon Exploration and Field Development*, cp-286.

Anderson, E. M. (1942). The Dynamics of Faulting and Dyke Formation, with Special Applications to Great Britain. *Oliver and Boyd*, *66*(3), 1–42.

Billings, M. P. (1972). *Structural geology* (3rd ed.). Prentice-Hall.

Blanc, E. J. P., Allen, M. B., Inger, S., & Hassani, H. (2003). Structural styles in the Zagros Simple Folded Zone, Iran. *Journal of the Geological Society*, *160*(3), 401–412. https://doi.org/10.1144/0016-764902-110

Bles, J. ., & Feuga, B. (1986). *The fracture of rocks*. North Oxford Academic Publishers.

Dunnington, H. V. (1958). Generation, accumulation and dissipation of oil in Northern Iraq. In, LG Weeks (Ed.) Habitat of Oil. *American Association of Petroleum Geologists Bulletin*, 1194–1251.

Engelder, T., & Geiser, P. (1980). On the use of regional joint sets as trajectories of paleostress fields during the development of the Appalachian Plateau, New York. *Journal of Geophysical Research: Solid Earth*, *85*(B11), 6319–6341.

Falcon, N. L. (1969). Problems of the relationship between surface structure and deep displacements illustrated by the Zagros Range. *Geological Society, London, Special Publications*, *3*(1), 9–21.

Fleuty, M. J. (1964). The description of folds. *Proceedings of the Geologists' Association*, *75*(4), 461–492. https://doi.org/https://doi.org/10.1016/S0016-7878(64)80023-7

Fossen, H. (2010). *Structural Geology*. Cambridge University Press.

Fouad, S. F. (2015). TECTONIC MAP OF IRAQ, SCALE 1: 1000 000, 3rd EDITION, 2012. *Iraqi Bulletin of Geology and Mining*, *11*(1), 1–7.

Ghasemi, A., & Talbot, C. J. (2006). A new tectonic scenario for the Sanandaj–Sirjan Zone (Iran). *Journal of Asian Earth Sciences*, *26*(6), 683–693.

Hancock, P. L. (1985). Brittle microtectonics: principles and practice. *Journal of Structural Geology*, *7*(3–4), 437–457.

Hancock, P. L., & Atiya, M. S. (1979). Tectonic significance of mesofracture systems associated with the Lebanese segment of the Dead Sea transform fault. *Journal of Structural Geology*, *1*(2), 143–153.

Ibrahim, A. O. (2009). *Tectonic Style and Evolution of the NW Segment of The Zagros Fold-Thrust Belt, Sulaimani Governorate, Kurdistan Region, NE Iraq*. University of Sulaimani.

Jassim, S. Z., & Goff, C. J. (2006). Geology of Iraq, Published by Dolin, Prague and Moravian. *Museum, Brno*, *341*.

Kent, W. N. (2010). Structures of the Kirkuk Embayment, northern Iraq: foreland structures or Zagros Fold Belt structures. *GeoArabia*, *15*(4), 147–188.

Mandl, G. (2005). *Rock Joints, The Mechanical Genesis*. Springer.

Ramsay, J. G., & Huber, M. I. (1987). Modern structural geology. *Folds and Fractures*, *2*, 309–700.

Sharland, P. R., Archer, R., Casey, D. M., Davies, R. B., Hall, S. H., Heward, A. P., Horbury, A. D., & Simmons, M. D. (2001). Arabian plate sequence stratigraphy, GeoArabia Spec. *Publ., Bahrain: Gulf Petrolink*, *2*, 374.

Sulaiman Al-Hakari, S. H., Tokmachi, O., & Abdalla, A. (2020). Paleostress Analysis from Fractures in Kalosh Anticline, Kurdistan Region, North–East of Iraq. *Geotectonics*, *54*, 821–831.

Taha, M. A., Al-Saddi, S. N., & Ibrahim, I. S. (1995). Microtectonic Study of Dokan Area, NE Iraq. *Iraqi Geol. Soc. Jour*, *28*(1), 25–35.

Talbot, C. J., & Alavi, M. (1996). The past of a future syntaxis across the Zagros. *Geological Society, London, Special Publications*, *100*(1), 89 LP – 109. https://doi.org/10.1144/GSL.SP.1996.100.01.08

van der Pluijm, B. A., & Marshak, S. (2004). *Earth Structure: An Introduction to Structural Geology and Tectonics, 2nd ed.(Norton: New York).*

Weinberger, R., Eyal, Y., & Mortimer, N. (2010). Formation of systematic joints in metamorphic rocks due to release of residual elastic strain energy, Otago Schist, New Zealand. *Journal of Structural Geology*, *32*(3), 288–305.

About the authors

Jihad H. Majeed is an Assistant Lecturer in the Department of Geology at the College of Science, University of Sulaimani, Kurdistan Region, Iraq. He earned his B.Sc. in Geology in 2011 and his M.Sc. in Structural Geology in 2023 from the same university. Before his current role, Jihad worked as a Demonstrator in the Geology Department from 2011 to 2020 and gained industry experience as a Field Engineer for Dana Gas Oil Company from 2018 to 2020. He now serves as a mentor, utilizing his expertise to guide students and support others in their academic and professional endeavors.

e-mail: jihad.majeed@univsul.edu.iq

Dr. Salim Hassan Suleiman Al-Hakari obtained a bachelor's degree from the University of Mosul in 1989 and a master's degree from the same university in 1993 in the field of structural geology in the subject of paleostress analysis. His first employment was as an assistant lecturer at the University of Sulaimani in 2004, then he obtained a Ph.D. from the University of Sulaimani in 2011 in structural geology in the subject of the geometry of the folds surrounding Sulaymaniyah city. He is now an assistant professor in structural geology at the same university. He has conducted numerous research papers about paleostress analysis and geometry of the folds.

email: Salim.sulaiman@univsul.edu.iq